

# Strength development of mortars containing ground granulated blast-furnace slag: Effect of curing temperature and determination of apparent activation energies

S.J. Barnett\*, M.N. Soutsos, S.G. Millard, J.H. Bungey

*Department of Civil Engineering, University of Liverpool, Brownlow Street, Liverpool, L69 3GQ, UK*

Received 9 February 2005; accepted 7 November 2005

## Abstract

The strength development of mortars containing ground granulated blast-furnace slag (ggbfs) and portland cement was investigated. Variables were the level of ggbfs in the binder, water–binder ratio and curing temperature. All mortars gain strength more rapidly at higher temperatures and have a lower calculated ultimate strength. The early age strength is much more sensitive to temperature for higher levels of ground granulated blast-furnace slag. The calculated ultimate strength is affected to a similar degree for all ggbfs levels and water–binder ratios, with only the curing temperature having a significant effect. Apparent activation energies were determined according to ASTM C1074 and were found to vary approximately linearly with ggbfs level from 34 kJ/mol for portland cement mortars to around 60 kJ/mol for mortars containing 70% ggbfs. The water–binder ratio appears to have little or no effect on the apparent activation energy.

© 2005 Elsevier Ltd. All rights reserved.

**Keywords:** Temperature; Compressive strength; Granulated blast-furnace slag; Apparent activation energy

## 1. Introduction

Ground granulated blast-furnace slag (ggbfs) is commonly used in combination with portland cement in concrete for many applications [1,2]. Concrete made with ggbfs has many advantages, including improved durability, workability and economic benefits [1]. The drawback in the use of ggbfs concrete is that its strength development is considerably slower under standard 20 °C curing conditions than that of portland cement concrete, although the ultimate strength is higher for the same water–binder ratio [3–5]. Ground granulated blast-furnace slag is not therefore used in applications where high early age strength is required. However, hydration of ggbfs is much more sensitive to temperature than portland cement and there is evidence that at higher early age temperatures, the strength development of ggbfs concrete is significantly enhanced [4,5]. In the construction of large structural concrete elements where heat dissipation is slow, there can be a significant rise in temperature within the first few days after casting due to the exothermic

reaction of the binder [6]. This leads to higher early age strengths, which can only be determined by temperature matched curing. Cubes or cylinders cured at 20 °C would underestimate the strength in the structure.

The work described here forms part of a research programme on the use of supplementary cementitious materials in fast-track concrete construction where high early age strengths are needed [7]. The major factors affecting the early age strength development of concrete are:

- concrete mixture composition, including factors such as water–binder ratio and the use of supplementary cementitious materials like ggbfs;
- type of formwork and size of structural element; and
- environmental conditions.

In order to investigate the effect of the curing temperature on the strength development of portland cement/ggbfs combinations, mortars have been prepared with a range of portland cement:ggbfs ratios (0, 20, 35, 50 and 70% ggbfs). Three different water–binder ratios were used at each replacement level, corresponding to concretes with 28-day target mean

\* Corresponding author. Tel.: +44 151 794 5230; fax: +44 151 794 5218.

E-mail address: [barnett@liv.ac.uk](mailto:barnett@liv.ac.uk) (S.J. Barnett).

strengths of 40, 70 and 100 N/mm<sup>2</sup>. The strength development of these mortars at curing temperatures of 10, 20, 30, 40 and 50 °C was determined and the apparent activation energies were calculated according to ASTM C1074 [8]. The apparent activation energy will be used to account for the temperature sensitivity of the binder hydration in modelling the strength development of concrete.

## 2. Experimental procedure

Mortars equivalent to concrete mixtures under investigation as part of a larger project [9,10] were prepared. The mixture proportions of these mortars were calculated from the concrete mixture proportions according to the requirements of ASTM C1074 [8]. The mortars had the same water–binder ratio as the concrete and the sand–binder ratio was equal to the coarse aggregate–binder ratio of the concrete. Where a superplasticising admixture (SPA) was used in the concrete, this was also included in the mortar mixture in the same proportion. The resulting mortar mixture proportions are presented in Table 1.

A single batch of portland cement was used for all mortars, provided by Castle Cement Limited. The ggbs came from a single batch provided by Frodingham Cement Limited. Chemical analysis of these materials is given in Table 2. The fine aggregate was a natural sand with 81% passing a 600 µm sieve. The sand was oven dried before use and allowance was made for 2.6% water absorption when calculating batch quantities for mixing. In mixtures with w/b ≤ 0.4, a polycarboxylate based superplasticising admixture, Structuro 111X provided by Fosroc Limited, was used.

A quantity of 0.015 m<sup>3</sup> of each mortar mixture was prepared in a horizontal pan mixer. Materials were added in the order: cement/ggbs, sand and the superplasticiser mixed with the water. The mortar was mixed for 3 min and then cast into steel 50 mm cube moulds. The specimens were consolidated on a vibrating table and wrapped in polyethylene film. They were then transferred to water tanks for curing at 20, 30, 40 and

Table 2

Chemical analysis of materials

Component	Portland cement %	GGBS %
SiO <sub>2</sub>	21.07	35.35
Al <sub>2</sub> O <sub>3</sub>	5.00	14
Fe <sub>2</sub> O <sub>3</sub>	2.92	0.36
CaO	64.40	41.41
MgO	2.07	7.45
SO <sub>3</sub>	2.65	0.1
K <sub>2</sub> O	0.59	–
Na <sub>2</sub> O	0.26	–
LOI	1.19	0.31
Insoluble	0.41	0.21
Cl	0.05	0.02
Free Lime	1.70	–
% Glass	–	97

50 °C. For curing at 10 °C, the specimens were wrapped in damp hessian and stored in an incubator. The specimens were demoulded at the time of the first compressive strength test. Three cubes were tested at six to eight testing ages for each mixture/temperature combination. In each case, the first testing age was chosen to correspond to a compressive strength of approximately 4 N/mm<sup>2</sup>. Subsequent tests were carried out at twice the age of the previous test.

## 3. Strength development

The compressive strength development with age at different curing temperatures is shown in Fig. 1 for three mortars (PC, 35% ggbs and 70% ggbs mixtures) at the high water–binder ratio. As expected, the strength development of all the mortars depended on the curing temperature. At early ages, the strength was higher at higher temperatures since the rate of reaction is greater. At later ages, the strength was lower at high curing temperatures. This is believed to be due to the formation of dense hydrated phases around the unreacted cement particles, preventing further hydration. The non-uniform distribution of hydration products also leads to larger pores in the microstructure. The mortars containing high levels of ggbs were more dependent on temperature, with the early age strengths showing a wider variation with temperature as the ggbs level increased. After 3 days, the portland cement mortar shown in Fig. 1(a) had strengths varying from 15 to 24 N/mm<sup>2</sup>. Note that the highest 3-day strength for the portland cement mortar was observed at 40 °C. The mortar with 70% ggbs (Fig. 1(c)) achieved a 3-day compressive strength of 26 N/mm<sup>2</sup> when cured at 50 °C but only 2 N/mm<sup>2</sup> at 10 °C.

The development of compressive strength,  $S$ , at a given curing temperature, can be described as a function of time,  $t$ , by the equation [10,11]:

$$S = \frac{S_{\infty}k(t - t_0)}{1 + k(t - t_0)} \quad (1)$$

where

$S_{\infty}$  calculated ultimate strength of the mortar, N/mm<sup>2</sup>  
 $t_0$  time at which strength development is assumed to begin, hours  
 $k$  rate constant, h<sup>−1</sup>

Table 1  
Mortar mixture proportions

Category	% GGBS	kg/m <sup>3</sup>					Free water/binder
		PC	GGBS	Free water	Sand (SSD)	SPA	
High w/b	0	415	–	249	1536	–	0.60
	20	321	81	249	1549	–	0.62
	35	272	146	242	1541	–	0.58
	50	205	205	250	1541	–	0.61
	70	137	319	237	1506	–	0.52
Intermediate w/b	0	462	–	185	1552	3.7	0.40
	20	373	94	182	1551	1.7	0.39
	35	315	170	175	1540	2.5	0.36
	50	236	236	181	1546	1.55	0.38
	70	140	327	182	1551	1.6	0.39
Low w/b	0	553	–	143	1501	14.4	0.26
	20	449	112	139	1498	8	0.25
	35	365	197	139	1498	4.9	0.25
	50	280	280	142	1496	8	0.25
	70	169	393	139	1498	4	0.25

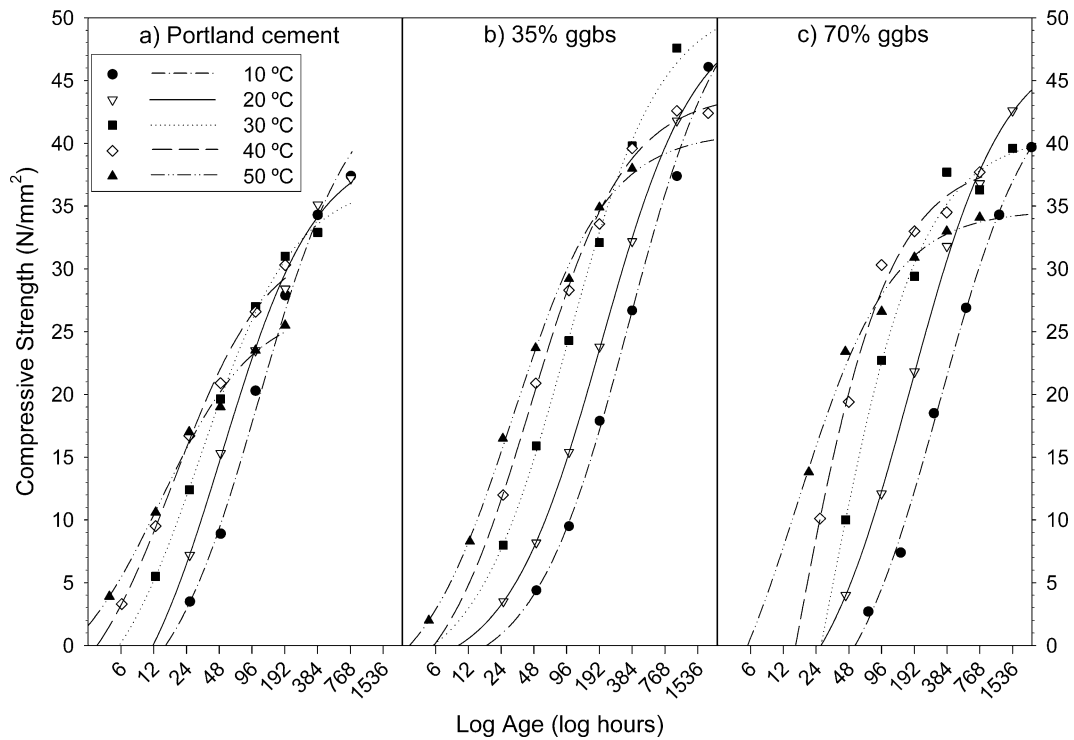


Fig. 1. Strength development of high w/b mortars at different curing temperatures.

The reciprocal of the rate constant  $k$  is the age beyond  $t_0$  at which the strength reaches 50% of the calculated ultimate strength. The values of  $S_\infty$ ,  $t_0$  and  $k$  were obtained for each curing temperature by regression analysis using Sigmaplot®. The best fit curves obtained are shown in Fig. 1.

The effect of ggbs level on the relative compressive strength,  $S/S_\infty$ , after 3 days is shown in Fig. 2 for all the mortars. At lower temperatures, the relative strength after 3 days was highly dependent on the ggbs level with higher ggbs levels reducing the relative compressive strength.

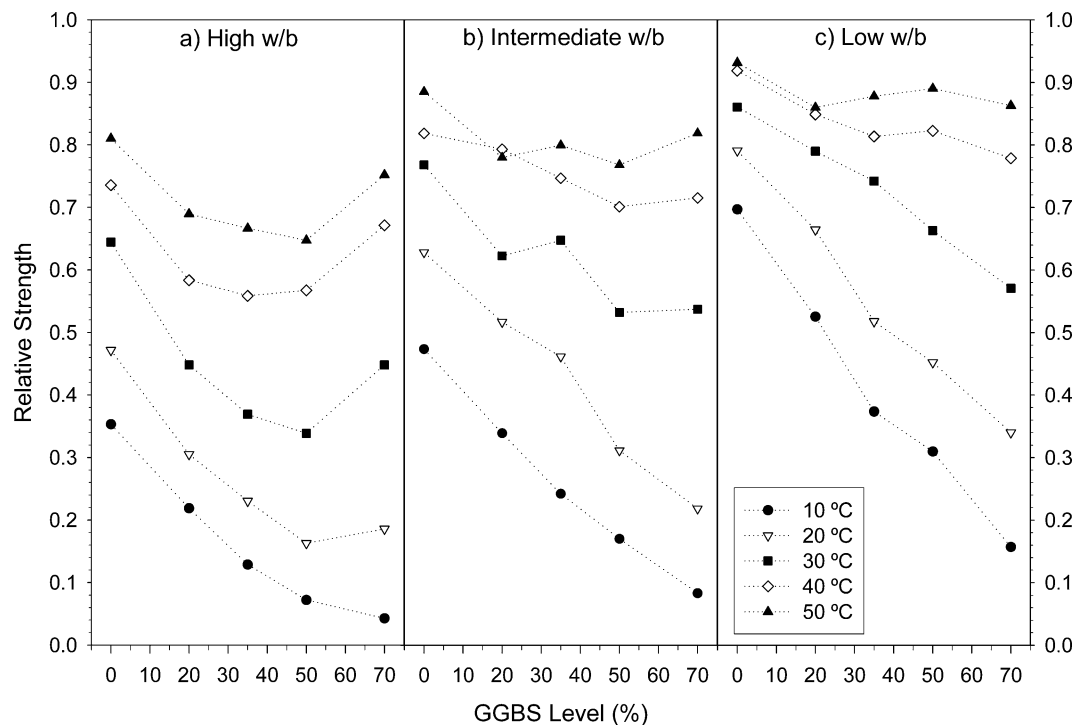


Fig. 2. Effect of GGBS level on 3-day relative compressive strength of mortars.

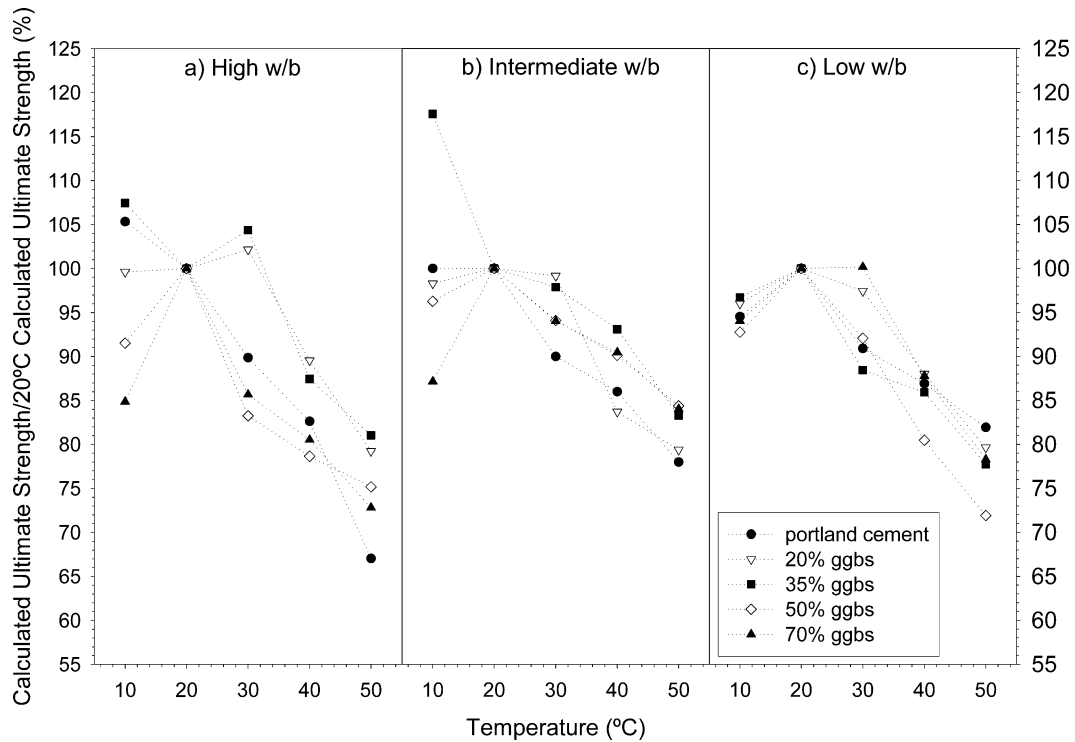


Fig. 3. Dependence of calculated ultimate strength of mortars on curing temperature.

However, at higher temperatures, the 3-day relative strength showed less dependence on ggbs level. At 40 and 50 °C, there is very little dependence on ggbs level and the relative strength of ggbs mortars at 3 days is approximately equivalent to that of portland cement mortars. For all ggbs levels, the relative strength at 3 days is increased at lower water–binder ratios.

The calculated ultimate strength,  $S_{\infty}$ , is plotted as a ratio of the 20 °C value for each mortar in Fig. 3. Generally, the calculated ultimate strength decreased with increasing temperature. No clear dependence was observed on the ggbs level and the calculated ultimate strength was affected to approximately the same degree for different water–binder ratios. In general the calculated ultimate strength was around 30% lower at 50 °C

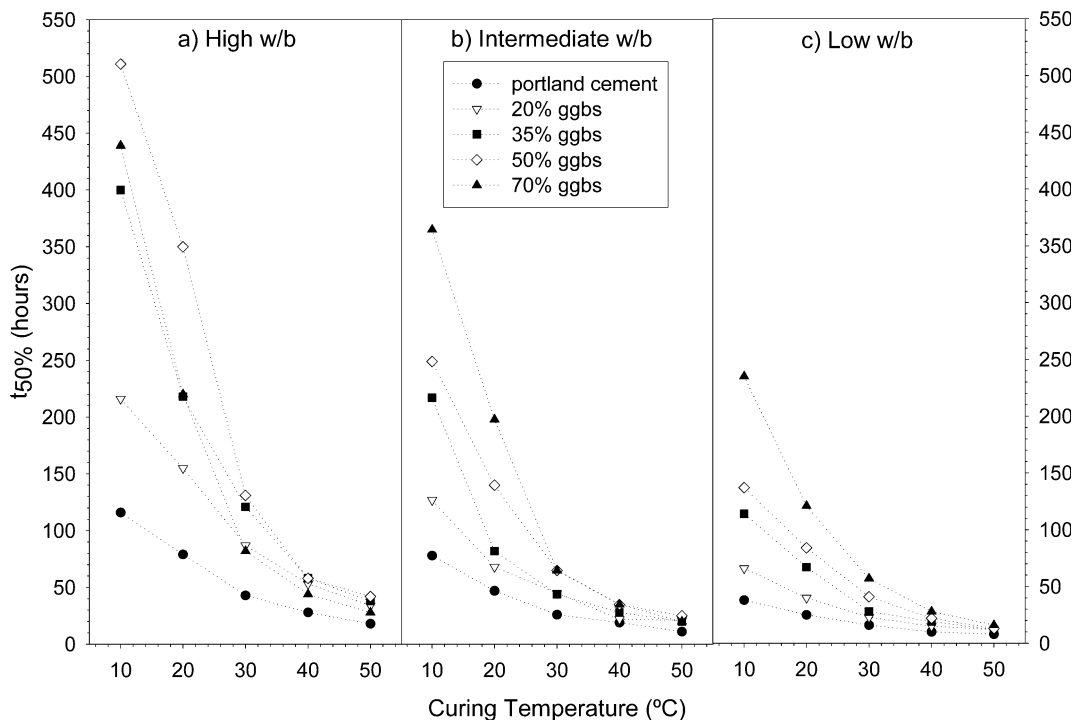


Fig. 4. Effect of curing temperature on the time taken to reach 50% of ultimate strength.

than at 20 °C. Many of the results for curing at 10 °C appear to be inconsistent with the trends observed at higher temperatures. It is believed that this is due to errors in calculation of the ultimate strength at 10 °C by regression analysis, because the strength is still increasing at the last testing age (see Fig. 1). Later testing at low temperatures would be desirable in order to obtain more accurate values for the true ultimate strength.

Fig. 4 shows the dependence on temperature of the time  $t_{50}$  at which each mortar reached 50% of its calculated ultimate strength. This value was calculated in each case from the parameters  $t_0$  and  $k$  obtained above:

$$t_{50} = t_0 + \frac{1}{k}. \quad (2)$$

This time increased with decreasing temperature, increasing water–binder ratio and increasing ggbs level. This figure clearly illustrates the benefits of higher curing temperatures on the early age strength development of mortars or concretes containing ggbs. At 10 °C, mortars containing high levels of ggbs took up to five times longer to reach 50% of their ultimate strength than portland cement mortars. However, at 50 °C the difference is much smaller, with all the mortars reaching 50% strength within 2 days and within 1 day for the lower water–binder ratios. The improvement between 20 and 30 °C for mortars containing high ggbs levels is particularly significant in terms of utilising ggbs in fast track construction, indicating that significant increases in early age strength development can be achieved if the in situ temperature rises by even a small amount above the standard curing temperature. For 50% and 70% ggbs levels, the time taken to reach 50% of ultimate strength at 30 °C was halved at all water–binder ratios, compared with curing at 20 °C.

#### 4. Determination of apparent activation energies

There are a number of functions available to describe the variation of the rate constant  $k$  with temperature. The Nurse–Saul maturity model [12,13] assumes a linear relationship:

$$M = \sum (T - T_0) \Delta t \quad (3)$$

and

$$k = a(T - T_0) \quad (4)$$

where

$M$  Nurse–Saul maturity, °C-h

$T$  temperature, °C

$T_0$  datum temperature, °C

$a$  is a constant.

The datum temperature is the temperature below which it is assumed that no strength gain will occur, taken as –11 °C in this work. The relationship between strength and maturity is assumed to be independent of temperature history, and can therefore be determined at a reference temperature. An equivalent age,  $t_e$ , can be defined as the age at the reference temperature at which the concrete has the same strength as at a time  $t$ :

$$t_e = \sum_t \frac{(T - T_0)}{(T_{ref} - T_0)} \Delta t. \quad (5)$$

An age conversion factor [14] can also be defined as follows:

$$\alpha = \frac{T - T_0}{T_{ref} - T_0} = \frac{k}{k_{ref}} \quad (6)$$

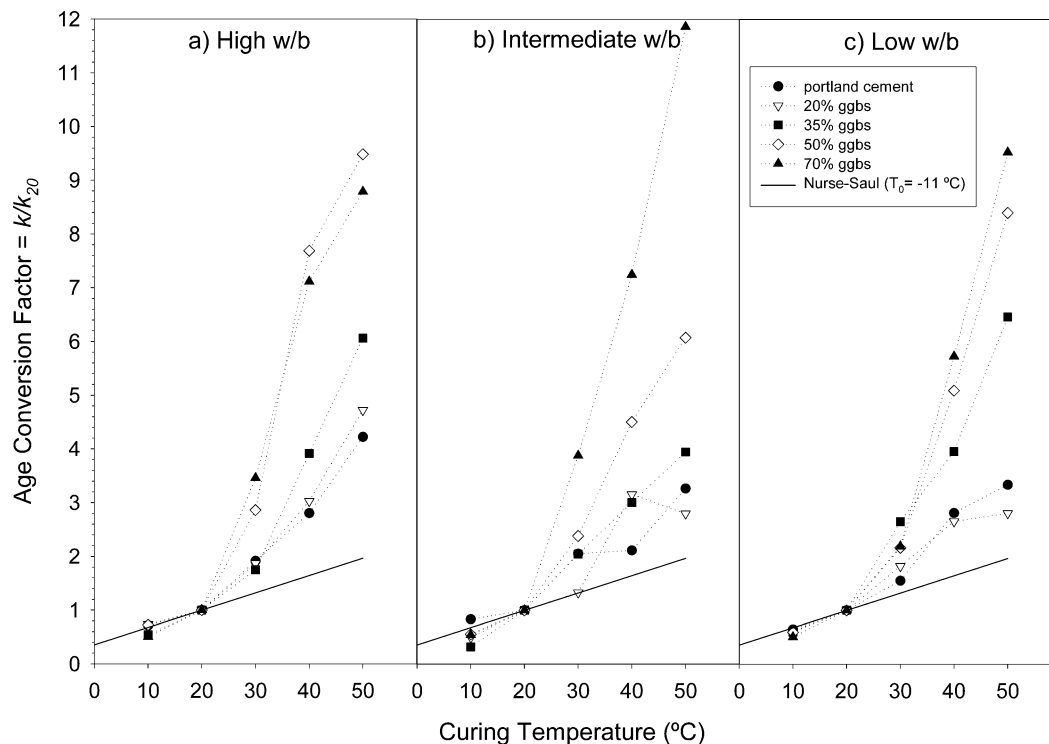


Fig. 5. Effect of curing temperature on age conversion factor.

The variation of the rate constant  $k$  with temperature  $T$  can also be described by the Arrhenius equation [10–12]:

$$k(T) = A \exp \left[ \frac{-E_a}{R(T + 273)} \right] \quad (7)$$

where

$A$  a constant,  $\text{h}^{-1}$

$E_a$  apparent activation energy,  $\text{J mol}^{-1}$

$R$  universal gas constant =  $8.314 \text{ J K}^{-1} \text{ mol}^{-1}$

In this case, the equivalent age is defined by [14,15]:

$$t_e = \sum_i \left( \exp \left[ \frac{E_a}{R} \left( \frac{1}{273 + T_{\text{ref}}} - \frac{1}{273 + T} \right) \right] \right) \Delta t. \quad (8)$$

And the age conversion factor as:

$$\alpha = \exp \left[ \frac{E_a}{R} \left( \frac{1}{273 + T_{\text{ref}}} - \frac{1}{273 + T} \right) \right] = \frac{k}{k_{\text{ref}}}. \quad (9)$$

The rate constant values obtained above were used to calculate the age conversion factors at different curing temperatures for each mortar, taking the reference temperature as  $20^\circ\text{C}$ . The age conversion factors obtained are plotted in Fig. 5. The age conversion factor increases exponentially with temperature. The linear relationship assumed by the Nurse–Saul model is inadequate to describe the variation of  $k$  with temperature for all the mortars. The deviation from linear behaviour is greater at higher ggbs levels.

The apparent activation energy of each mortar was determined, assuming the rate constant varied with tempera-

Table 3

Apparent activation energies of GGBS mortars

% GGBS	$E_a$ , kJ/mol		
	High w/b	Intermediate w/b	Low w/b
0	34.8	35.1	32.9
20	36.6	35.2	36.8
35	47.1	47.0	46.8
50	54.6	48.0	52.6
70	58.8	62.1	57.9

ture according to Eq. (7). According to this equation, the relationship for each mortar between  $\ln k$  and the reciprocal of absolute temperature (plotted in Fig. 6) is linear:

$$\ln k = \frac{-E_a}{RT} + \ln A. \quad (10)$$

Accordingly, the value of the apparent activation energy can be calculated for each mortar from the slopes of the best-fit straight lines shown in Fig. 6. Note that for the 20% ggbs mortar at the low water–binder ratio (Fig. 6(c)), the rate constant obtained at  $50^\circ\text{C}$  has been excluded from the regression as an outlier.

The values of  $E_a$  obtained are shown in Table 3 and plotted in Fig. 7. The apparent activation energy was relatively independent of water–binder ratio and depended primarily on the percent ggbs in the binder. The apparent activation energy was highly dependent on the ggbs level, with high replacement levels leading to higher apparent activation energies. The apparent activation energy obtained for portland cement was 34 kJ/mol. The apparent activation energy increases approximate-

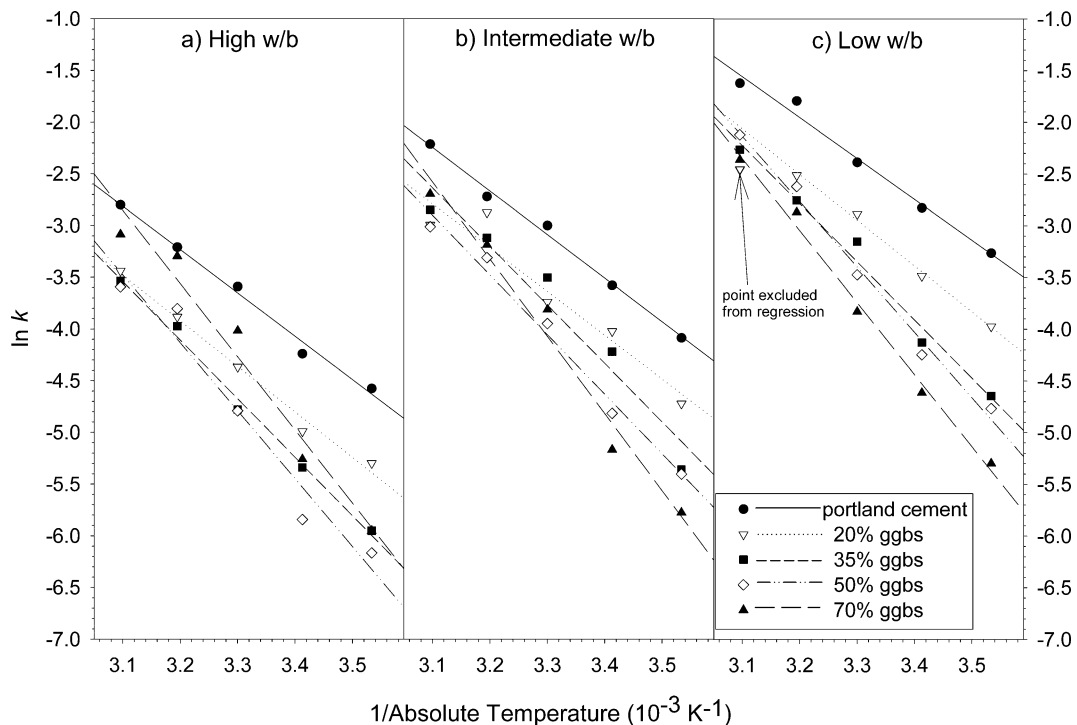


Fig. 6. Effect of curing temperature on rate constant  $k$ .



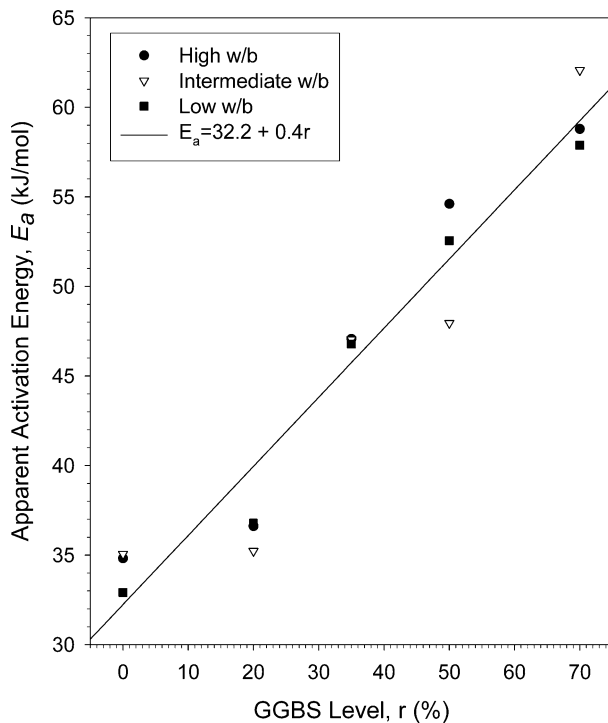


Fig. 7. Apparent activation energies of mortars.

ly linearly with increasing ggbs level to a value of around 60 kJ/mol for the 70% ggbs mortars.

## 5. Conclusions

The early age strength development of mixtures containing ggbs is highly dependent on temperature. Under standard curing conditions, ggbs mortars gain strength more slowly than portland cement mortars. However, at higher temperatures, strength gain is much more rapid and the improvement in early age strength is more significant at higher levels of ggbs. Even a 10 °C increase in curing temperature above standard curing temperature considerably accelerates the strength development of mortars containing high levels of ggbs (Fig. 4) and at 40 and 50 °C, the strength of ggbs mortars is more or less equivalent to that of portland cement mortar after 3 days (Fig. 3).

This increased temperature sensitivity of the strength gain in ggbs mortars is reflected in their higher apparent activation energies. The apparent activation energy increases approximately linearly with ggbs level. The portland cement used in this work has an apparent activation energy of 34 kJ/mol while this figure increases to 60 kJ/mol when a binder consisting of 70% ggbs and 30% portland cement was used. These values are in broad agreement with values quoted in the literature [11,16,17].

The apparent activation energies obtained in this work are currently being used to predict concrete strength development under variable temperature conditions. Initially, existing models [12–17], which generally have been based on portland cement hydration only, are being assessed for their suitability in modelling strength development of concrete containing ggbs.

## Acknowledgements

The authors would like to acknowledge the financial support of the Engineering and Physical Sciences Research Council (EPSRC GR/R83880/01) and Appleby Group Limited. Materials were kindly provided by Frodingham Cement, Castle Cement and Fosroc Limited. We would also like to thank Mr D. Hunter (University of Liverpool) for his contribution to the experimental part of this work.

## References

- [1] Report of ACI Committee 233, Slag Cement in Concrete and Mortar, ACI 233R-03, American Concrete Institute, Farmington Hills, Mich, 2003.
- [2] J. Bijen, Blast Furnace Slag Cement for Durable Marine Structures, Stichting BetonPrisma, Netherlands, 1996.
- [3] J.I. Escalante-García, J.H. Sharp, The microstructure and mechanical properties of blended cements hydrated at various temperatures, *Cem. Concr. Res.* 31 (2001) 695–702.
- [4] J.I. Escalante, L.Y. Gómez, K.K. Johal, G. Mendoza, H. Mancha, J. Méndez, Reactivity of blast-furnace slag in portland cement blends hydrated under different conditions, *Cem. Concr. Res.* 31 (2001) 1403–1409.
- [5] D.M. Roy, G.M. Idorn, Hydration, structure and properties of blast furnace slag cements, mortars and concrete, *ACI Journal* 79 (6) (1982) 444–457.
- [6] J.G. Sanjayan, B. Sioulas, Strength of slag-cement concrete cured in place and in other conditions, *ACI Mater. J.* 97 (5) (2000) 603–611.
- [7] S.J. Barnett, M.N. Soutsos, J.H. Bungey, S.G. Millard, Fast-track concrete construction using cement replacement materials, in: V.M. Malhotra (Ed.), *Proceedings of the Eighth CANMET/ACI International Conference on Fly Ash, Silica Fume, Slag, and Natural Pozzolans in Concrete*, ACI SP-221, American Concrete Institute, Farmington Hills, Mich, 2004, pp. 135–151.
- [8] ASTM C1074-98, Standard practice for estimating concrete strength by the maturity method, *Annual Book of ASTM Standards Volume 04 02 Concrete and Aggregate*, 1999.
- [9] S.J. Barnett, M.N. Soutsos, J.H. Bungey, S.G. Millard, The effect of the level of cement replacement with ground granulated blastfurnace slag on the strength development and adiabatic temperature rise of concrete mixtures, in: R.K. Dhir (Ed.), *Proceedings of Global Construction: Ultimate Concrete Opportunities, Event 1: Cement Combinations for Durable Concrete*, Dundee, UK, 2005 (July), pp. 165–172.
- [10] M.N. Soutsos, S.J. Barnett, J.H. Bungey, S.G. Millard, Fast track construction with high strength concrete mixes containing ground granulated blast furnace slag, in: H.G. Russell (Ed.), *Proceedings of ACI Seventh International Symposium on High Strength/High Performance Concrete*, ACI SP-228, vol. 1, 2005, pp. 255–270.
- [11] R.C. Tank, N.J. Carino, Rate constant functions for strength development of concrete, *ACI Mater. J.* 88 (1) (1991) 74–83.
- [12] R.W. Nurse, Steam curing of concrete, *Mag. Concr. Res.* 1 (2) (1949) 79–88.
- [13] A.G.A. Saul, Principles underlying the steam curing of concrete at atmospheric pressure, *Mag. Concr. Res.* 2 (6) (1951) 127–140.
- [14] N.J. Carino, The maturity method, in: V.M. Malhotra, N.J. Carino (Eds.), *CRC Handbook on Nondestructive Testing of Concrete*, 2nd edition, CRC Press, 2004.
- [15] P. Freiesleben Hansen, J. Pedersen, Maturity computer for controlled curing and hardening of concrete, *Nord. Betong* 1 (1977) 19–34.
- [16] K.O. Kjellsen, R.J. Detweiler, Later-age strength prediction by a modified maturity model, *ACI Mater. J.* 90 (3) (1993) 220–227.
- [17] G. Chanvillard, L. D'Aloia, Concrete strength estimation at early ages: modification of the method of equivalent age, *ACI Mater. J.* 94 (6) (1997) 520–530.